Effect of Anharmonicities on the Thermodynamic Properties of the Water Dimer†

Camelia Muñoz-Caro* and Alfonso Niño

E.U. Informática de Ciudad Real, Universidad de Castilla−La Mancha, Ronda de Calatrava 5, 13071 Ciudad Real, Spain

Received: January 6, 1997; In Final Form: March 21, 1997[⊗]

A study of the effect of anharmonicities and large amplitude vibrations on the thermodynamic properties of the water dimer is presented. Different vibrational models have been constructed using ab initio data obtained at the MP2(Full)/6-311++G(2d,2p) level. In particular, we present the first complete analysis of the rotation of the hydrogen donor monomer around the O···O axis. The potential barrier was found to be 221 cm^{-1}. A variational calculation of the torsional energy levels yields a fundamental frequency of 105 cm^{-1}. The O···O stretching mode is described using a Morse function. The fundamental frequency and the dimerization energy are calculated to be 153 cm^{-1} and 5.15 kcal/mol, respectively, in agreement with the experimental results. For the dimerization reaction we have calculated ΔS, ΔH, and the equilibrium constant, K_p. The results show that inclusion of anharmonicity into the vibration modes favors the lower experimental limit for ΔS and the upper limit for ΔH. In addition, the anharmonic corrections reduce the difference between calculated and experimental K_p. This difference decreases with temperature. A high-temperature limit of 3.47×10^{-5} atm^{-1} was found for K_p.

Introduction

The accurate prediction of thermodynamic properties using a pure theoretical basis is of great interest in modern chemistry. The direct approach is exemplified by the computation of gas phase enthalpy changes. The magnitude of these changes can be determined by computing the internal energy of the system and the change in mechanical energy, $\Delta(pV)$ factor. The internal energy can be calculated by ab initio methodology through the computation of the total electronic energy, the zero-point vibrational energy, and the changes in vibrational, rotational, and translational energies at the considered temperature.[1] However, only enthalpy can be computed in this direct form. In addition, an accurate determination of internal energy from ab initio calculations needs large basis sets and to account for the correlation energy. From a practical standpoint these requirements are translated into large amounts of time and computational resources for even moderate size molecules.

A more general approach to the computation of equilibrium properties is based on statistical mechanics. Thus, any thermodynamic property can be computed using the partition function, which incorporates all the energy states of the molecule. In this form, it is possible to derive a functional relationship between the molecular structure and a macroscopic, equilibrium property. For an ideal gas, the nuclear, electronic, and translational contributions to the partition function can be easily determined.[2] The vibrational and rotational contributions are usually calculated using the rigid rotor−harmonic oscillator approach. In this form, the derivation of equilibrium properties is straightforward.[2] The technique is implemented in several popular quantum mechanical software packages.[3] However, the existence of nonrigidity invalidates the harmonic approximation. Nonrigidity appears when several energetically accessible minima exist on the potential hypersurface,[4] and it is associated with large amplitude, anharmonic vibrations, such as inversions and internal rotations. Large amplitude modes are poorly described by the harmonic approximation, which assumes a pure quadratic dependence of the nuclear potential with the vibrational coordinates.[5] In addition, when a molecule undergoes large amplitude vibration the vibrational kinetic term may change significantly, and it is necessary to account for its dependence on the vibrational coordinates.

Nonrigidity is related to inter- and intramolecular hydrogen bonding due to the flatness of the potential hypersurface on the coordinates involved in the hydrogen bond.[6] This fact is translated into very soft vibrational modes and therefore, into anharmonicity and large amplitude motions. Since the vibrational energy levels appear as negative exponents in the partition function, accurate descriptions of low-frequency vibrations are necessary for a reliable computation of equilibrium properties using the statistical approach.

We have selected the water dimer for analyzing the effect of anharmonicity and large amplitude motions on the thermodynamics of hydrogen-bonded complexes. The water dimer is the prototype of hydrogen-bonded complexes and has received considerable attention from both the theoretical and the experimental standpoints.[6b,c,7,8] However, the low concentration of dimers present in the water vapour (around 1% at 373 K and a pressure of 1 atm) makes accurate thermodynamic and spectroscopic measurements difficult.[7,9] Therefore, the theoretical evaluation of the thermodynamic properties for the dimerization reaction is of interest.

Formation of hydrogen-bonded complexes from two monomers converts three rotational and three translational degrees of freedom into six new intermolecular modes of low frequency. In the water dimer, one of these modes is the hindered rotation of the donor monomer around the O···O axis. The effect of this torsion on the thermodynamic functions has been considered in previous work[10,11] using the Pitzer method. However, in this approach, the kinetic term is considered to be constant with the vibrational displacement and the potential function is rigid, corresponding only to the first term of a Fourier expansion. No detailed analysis for this mode has been provided so far.

On the other hand, an important feature in the vibrational behavior of a H-bonded complex, X−H···Y, is the interaction between the X−H stretching of the hydrogen donor molecule and the X···Y stretching. These two modes are strongly

† This work is dedicated to the memory of Prof. Federico Peradejordi.

* Corresponding author. E-mail: cmunoz@inf-cr.uclm.es.

[⊗] Abstract published in *Advance ACS Abstracts,* May 1, 1997.

S1089-5639(97)00134-5 CCC: $14.00

coupled,[12] and they have been extensively studied by IR and rotational spectroscopy in different compounds.[13] An adiabatic model has been applied to the study of these motions. In this model the low-frequency vibration contributes to the potential with a harmonic term and moves in an average potential generated by the high-frequency mode.[12] Kinetic and potential couplings are not explicitly considered. Variational models, including potential coupling, can also be found in the literature.[14] However, these models do not include the effect of the kinetic coupling, and they use internal coordinates as vibrational coordinates.

In this paper we investigate the effect of anharmonicities on the thermodynamics of the dimerization of water. Thus, anharmonic corrections are developed for different vibrational modes. In particular, the internal rotation around the O···O axis and the O···O stretching are considered. Also, the reliability of the usual two-dimensional models used for describing the stretching modes of hydrogen bonds is analyzed. The effect of these corrections on the values of ΔS, ΔH, and the association constant of water is discussed and compared to previous results.

Theory

The thermodynamic properties will be computed from the canonical partition function, Q,

$$Q = \sum_{i}^{\infty} \exp[-\epsilon_i/kT] \tag{1}$$

where the index runs on every energy state in the ensemble. For an ideal gas we have[2] $Q = q^N/N!$, for indistinguishable particles, where q is the molecular partition function and N represents the number of molecules in the ensemble. The molecular partition function, q, is factorized as a product of q_n, q_e, q_t, q_r, and q_v, corresponding to the nuclear, electronic, translational, rotational and vibrational partition functions.[2] At standard ambient temperature, only the ground nuclear and electronic states need to be considered. Thus, q_n is taken as unity and q_e as the ground electronic state degeneracy. The translational partition function, q_t, will be calculated with the usual closed form[2]

$$q_t = (2\pi MkT/h^2)^{3/2} \cdot V \tag{2}$$

where M represents the total mass of the molecule, k the Boltzman constant, h the Planck constant, T the absolute temperature, and V the volume.

The rotational contribution will be computed applying the semiclassical expression[2]

$$q_r = (\pi^{1/2}/\sigma)\,[(kT)^3/(A \cdot B \cdot C)]^{1/2} \tag{3}$$

where A, B, and C represent the overall rotational constants determined at the equilibrium geometry and σ is the symmetry number, i.e., the order of the rotational subgroup of the molecule.

The vibrational contribution, q_v, can be fully factorized as a product of $3N-6$ partial partition functions

$$q_v = \prod_{i}^{3N-6} [\sum_{j}^{\infty} \exp[-\epsilon_{ij}/kT]] \tag{4}$$

For a harmonic vibration, i, the contribution to eq 4 is calculated using the closed form[2]

$$q_v(i) = \exp[-\nu_0(i)/2kT]/(1 - \exp[-\nu_0(i)/kT]) \tag{5}$$

where the origin of energies is taken at the bottom of the potential well and ν_0 corresponds to the fundamental frequency of vibration.

The contribution of large amplitude vibrations to eq 4 will be obtained by direct summation of states, which are determined using the Hamiltonian for large range motions[15−17]

$$\hat{H} = \sum_{i}^{n} \sum_{j}^{n} \left(-B_{ij} \frac{\partial^2}{\partial q_i \partial q_j} - \frac{\partial B_{ij}}{\partial q_i} \frac{\partial}{\partial q_j} \right) + V(q_1, ..., q_n) \tag{6}$$

where n stands for the number of vibrations, q represents the vibrational coordinates and $B_{ij} = (\hbar^2/2)g_{ij}$ are the kinetic terms. The kinetic elements, B_{ij}, are obtained from the last $n \times n$ elements of the $3N \times 3N$ rotational−vibrational **G** matrix.[16,17] The potential energy function for eq 6 will be obtained, within the adiabatic approximation,[18] from the total energy results of accurate ab initio calculations. The potential functions will be described through Fourier or Taylor series on the vibrational coordinates.[19−22] These calculations are performed by fixing the internal coordinates in question and fully optimizing the remaining molecular parameters.[23] Equation 6 is then solved using a variational formalism previously proposed.[20] This formalism allows the vibrations to be described with different boundary conditions using hybrid free rotor + harmonic oscillator basis functions.[21,24]

The description of the slightly anharmonic vibrations can be improved from the harmonic approximation by a potential function that describes the potential hypersuface beyond the quadratic zone. Thus, we will apply an independent modes approach generating a potential function for finite displacements on the normal coordinate.[10,25] For a displacement, ΔW, in the W_i normal mode direction, the new Cartesian coordinates, $\mathbf{r}_i$, are obtained as

$$\mathbf{r}_i = \mathbf{r}_e + \Delta W_i \tag{7}$$

where $\mathbf{r}_e$ represents the equilibrium position. The potential energy can be expanded on ΔW, yielding

$$V_i(W) = \sum_{j=2} (1/j!)(\partial^j V_i/\partial W_i^j)_e \cdot \Delta W_i^j \tag{8}$$

Equation 8 represents a Taylor expansion of the potential energy around the equilibrium position in the direction of a normal coordinate. The coefficients of eq 8 will be obtained computing the potential energy for several points obtained at different increments ΔW. After construction of the potential function, the vibrational Hamiltonian will be solved variationally in the harmonic oscillator basis set. The contribution to eq 4 will be obtained by direct summation.

The reliability of the calculated partition function, eq 1, will be enhanced by introducing experimental information, when available, into ln Q, using the method described in ref 26. Thus, at constant pressure, ln Q is transformed into a simple function of the inverse of the absolute temperature, $Y = 1/T$, expanding in a Taylor series

$$\ln Q(T) = \sum_{i} A_i Y^i \tag{9}$$

with

$$A_i = (1/i!)(\partial^i \ln Q/\partial Y^i)_0 \tag{10}$$

Equation 10 is obtained by performing a least-squares fit of the theoretical ln Q values calculated for a set of Y points. The

TABLE 1: Kinetic Terms at the Equilibrium Position, *B*, Potential Functions ($V = V_2q^2 + V_3q^3 + V_4q^4$) and Fundamental Frequencies for the Water Monomer[a]

mode	sym.	B	V_2	V_3	V_4	ν_{har}[b]	ν_{anh}[c]	ν_{exp}[d]
ν_1	a_1	15.56	442 75.02	148 47.38	−294 15.68	1660	1620	1595
ν_2	a_1	16.14	232 034.83	−422 252.08	492 968.31	3870	3789	3652
ν_3	b_2	15.58	255 518.96		−100 422 0.44	3991	3785	3756

[a] The V_2 term corresponds to the harmonic approximation. Symmetry referred to the C_{2v} point group. All data in cm^{-1}. [b] This work, harmonic frequencies at the MP2(Full)/6-311++G(2d,2p) level. [c] This work, anharmonic frequencies. [d] Experimental data taken from ref 32.

experimental information is incorporated through minimizing the difference between the computed and observed values for several thermodynamic functions. Thus, considering N thermodynamic magnitudes, X, we build an error function

$$E(\mathbf{C}) = \sum_i^N (X^i(\mathbf{C})_c - X_o{}^i)^2 \qquad (11)$$

where $\mathbf{C}$ represents a vector composed by the A_i terms of eq 10. $X^i(\mathbf{C})_c$ and $X_o{}^i$ are the calculated and observed values for the function, respectively. To reduce the error, $E(\mathbf{C})$, we apply a quasi-Newton multidimensional minimization[27] with respect to the A_i parameters.[26] From a physical standpoint, the refinement introduces the effect of the coupling between motions not accounted for in the initial model. It also reflects the effect of intermolecular interactions not considered in the ideal gas approach used for Q.

After calculation of ln Q, the thermodynamic properties of interest for this study are obtained through the usual statistical expressions.[2]

Computational Details

The structural parameters, normal modes analysis, potential functions and kinetic energy terms for the water monomer and dimer are obtained from ab initio calculations using the triple split plus polarization and diffuse functions 6-311++G(2d,2p) basis set. This basis was selected because it has shown to be enough flexible to describe hydrogen-bonded complexes at the Hartree−Fock and correlated levels.[28] Correlation energy is accounted for at the all electrons MP2 level. All the calculations are carried out using the GAUSSIAN 94 package[3b] except for the normal modes analysis in internal coordinates that are performed using the GAMESS[3a] program. The fully optimized geometry of water dimer is obtained using the GAUSSIAN 94 "tight" option due to the existence of very soft vibrational modes. The rotational−vibrational **G** matrix and the kinetic terms for large amplitude vibrations are obtained using the KICO program.[29] The vibrational energy levels are variationally calculated with the NIVELON program.[30] Finally, the refinement of the partition function and the calculation of thermodynamic properties are performed with the PARTI program.[31]

Results and Discussion

Water Monomer. The water monomer is an extensively studied system. Thus, only the information needed for the construction of the canonical partition function will be provided. After full geometry optimization at the MP2(Full)/6-311++G(2d,2p) level, the A, B, and C rotational constants are found to be 820.4, 438.3, and 285.7 GHz respectively. The harmonic frequencies, computed after a normal modes analysis, are collected in Table 1. To evaluate the effect of anharmonicity in the partition function, anharmonic corrections are introduced in the vibration modes. These corrections are obtained by displacing the nuclei in the direction of the different normal coordinates. Thus, displacements of ±0.1 and ±0.2 on the normal coordinate are used for both the bending, ν_1, and symmetric stretching, ν_2, modes. Potential functions are obtained by fitting the results to a Taylor series on the vibrational coordinates. The kinetic terms, anharmonic potentials, and fundamental frequencies are shown in Table 1. It is found that anharmonic corrections reduce the error in the frequencies to 1.6% and 3.7% for the ν_1 and ν_2 modes, respectively. However, application of this approach to the asymmetric stretching mode, ν_3, results in a fundamental frequency higher than the harmonic value. This result is unphysical since the harmonic approximation overestimates the fundamental frequency at the SCF and correlated levels.[33] The problem can be analyzed in terms of the OH bond lengths variation. In the harmonic approximation the parabolic shape of the potential makes the increase or the decrease of the vibration coordinate equally probable. In the asymmetric stretching of water this fact is translated in a normal mode where the elongation of one OH bond equals the shortening of the other. However, a simple Morse potential shows that the contraction of a bond is more difficult than its elongation. Thus, a finite displacement of equal magnitude in both bonds leads to an increase of potential energy higher than in the harmonic case. This fact is translated in a positive quartic correction in the potential and, therefore, in an increase of the fundamental frequency. The problem can be solved considering the OH contraction amplitude with respect to the OH elongation as a parameter. This parameter is optimized in the ν_3 normal mode using internal coordinates.[34] For each value of the parameter, a potential function is derived and the fundamental frequency is calculated. Using a steepest descent approach, the difference between the experimental and calculated fundamental frequencies is reduced below 1%. Thus, we found that a reduction of 4% in the OH contraction yields a fundamental frequency of 3785 cm^{-1}, see Table 1.

From the rotational and vibrational information, we apply eqs 2, 3, and 5 to obtain the partition function, Q. Using Q, C_p and S° are statistically calculated[2] at 298.15 K and at a constant pressure of 1 atm. In the harmonic case, we obtain 33.36 and 188.47 J/(mol·K) for C_p and S°, respectively. In the anharmonic case, the results are C_p = 33.39 J/(mol·K) and S° = 188.48 J/(mol·K). These data can be compared to the experimental[35] 33.54 and 188.72 J/(mol·K) values for C_p and S°, respectively. The anharmonic results are only slightly better than the harmonic. The calculated internal and Gibbs energies are found to be 62.42 and 8.71 kJ/mol in the harmonic case whereas 64.38 and 10.66 kJ/mol are obtained in the anharmonic one. In this case, the difference increases up to 1.96 kJ/mol (0.47 kcal/mol).

For the study of the dimerization reaction, ln Q, $(\partial \ln Q/\partial T)$ and $(\partial^2 \ln Q/\partial T^2)$ are obtained from the anharmonic model for temperatures ranging from 273.15 to 373.15 K. The functions are fitted to $1/T$, eq 9 and it is found that third order polynomials in $1/T$ reproduce the data. From the experimental values 33.54 and 188.72 J/(mol·K) for C_p and S°, respectively, the functions are refined[26] until the difference between calculated and experimental values falls below 0.001 J/(mol·K).

Water Dimer. The hydrogen-bonded water dimer exhibits C_s symmetry. Thus, its 12 vibrational modes are classified as symmetric or antisymmetric (a′, a″) with respect to the symmetry

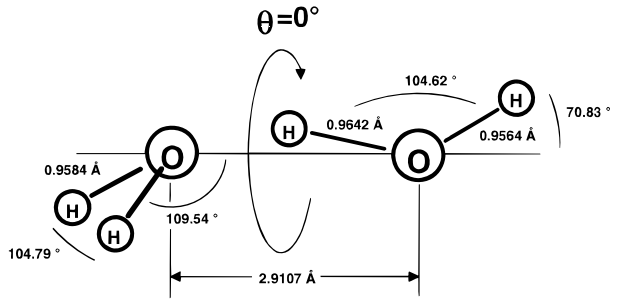

Figure 1. Fully optimized geometry of the water dimer at the MP2-(full)/6-311++G(2d,2p) level. θ refers to the torsional angle of the donor monomer around the O···O axis.

plane. In this work, the normal modes are numbered using the convention of Reimers et al.[36] A tightened full molecular geometry optimization was carried out at the MP2(Full)/6-311++G(2d,2p) level. The resulting structure is shown in Figure 1. At the equilibrium geometry the *A*, *B*, and *C* rotational constants are found to be 6.41, 6.41, and 217.75 GHz respectively. A normal modes analysis was performed. The harmonic frequencies are collected in Table 2. The table also shows the MP2/aug-cc-pVTZ[37] and MP2/[9,6,4,2/6,4,2][38] calculated frequencies and the available experimental values.

The six high-frequency modes, see Table 2, can be correlated with the three vibrations of the water monomers. Anharmonic corrections for these vibrations are obtained by displacement of 0.1 on the normal modes except for the ν_3 mode, the hydrogen donor O−H stretching, which will be described in a different form. The a″ symmetry ν_9 mode, the asymmetric stretching of the acceptor monomer, shows the same wrong behavior as the ν_3 mode of water. It is solved in the same way, i.e., introducing into the normal mode a difference of 4% in the bond variation. The anharmonic potentials, the kinetic terms and the computed fundamental frequencies are collected in Table 2. It is observed that the anharmonic corrections produce a decrease of the frequencies, approaching the experimental results. In particular, the calculated frequency for the ν_9 mode agrees to within 1.4−1.1% of the experimental data, Table 2. The ν_3 stretching mode is described through the O−H distance. Thus, a grid of points on the O−H bond length is performed from 0.9242 to 1.0442 Å in increments of 0.2 Å. At each fixed O−H value the geometry is fully optimized. The kinetic term, B_{OH}, is obtained through the rotational−vibrational **G** matrix.[16,17] Since the variation with the motion is found very small, the equilibrium value, $B_{OH} = 17.21$ cm^{-1}, will be used. The potential for the ν_3 vibration is constructed by fitting the total energy results to a Taylor series on the displacement coordinate, Δr_{OH}. Thus, we obtain (in cm^{-1})

$$V = 201\,000.50\cdot(\Delta r_{OH})^2 - 485\,478.37\cdot(\Delta r_{OH})^3 + 636\,271.61\cdot(\Delta r_{OH})^4 \quad (12)$$

with correlation coefficient $R = 1.00000$ and standard deviation $\sigma = 0.40$ cm^{-1}. The fundamental frequency is calculated variationally within the harmonic oscillator basis. Table 2 shows that the calculated frequency, 3548 cm^{-1}, is smaller than both the 3773 cm^{-1} harmonic result and the 3746 cm^{-1} found at the MP2/[9,6,4,2/6,4,2] level.[38] Table 2 also shows that our anharmonic result is closer to the 3480 cm^{-1} experimental value.

The first of the low-frequency modes, ν_{12}, is the hindered rotation of the donor monomer around the O···O axis. To describe this mode, we have performed a conformational analysis rotating the donor water molecule around the O···O axis. Thus, increments of 30° were used for the torsional angle, θ, with the origin conformation taken at the C_s symmetry equilibrium position, see Figure 1. The remaining internal coordinates were fully optimized at each point. Figure 2 shows the resulting potential as a function of the torsional angle, θ. A maximum is found in the C_1 symmetry $\theta = 150°$ conformation. This maximum can be attributed to steric hindrance between the hydrogens of the acceptor molecule and the free hydrogen of the donor monomer. A local minimum appears at $\theta = 180°$ in the C_s conformation where the projection of the donor free hydrogen lies between the two hydrogens of the acceptor. The barrier to rotation ($\theta = 150°$ conformation − $\theta = 0°$ conformation) is found 221 cm^{-1}. This result falls between the 0.67 kcal/mol (234 cm^{-1}) computed at the MP2/6-311+G(d,p) level and the 0.59 kcal/mol (206 cm^{-1}) computed without molecular relaxation at the MP4/6-311G+G(2df,2p) level.[6a] The energy points and the kinetic terms, B_θ, obtained from the rotational−vibrational **G** matrix[16,17], are fitted to Fourier expansions on the torsional angle. The kinetic and potential functions obtained are (in cm^{-1})

$$B_\theta = 34.30 - 1.51\cos(\theta) - 0.52\cos(2\theta) + 0.14\cos(3\theta)$$

$$V = 146.38 - 104.79\cos(\theta) - 38.56\cos(2\theta) - 3.03\cos(3\theta) \quad (13)$$

with $R = 0.999\,70$, $\sigma = 0.03$ cm^{-1} for B_θ and $R = 0.999\,80$, $\sigma = 1.90$ cm^{-1} for V. From these data the torsional energy levels are computed variationally in the free rotor basis. The results are collected in Table 3. The fundamental frequency is found to be 105 cm^{-1}. Table 2 shows that this value is smaller than the harmonic 135 cm^{-1} computed at the same level of theory and smaller than the 140 cm^{-1} obtained at the MP2/aug-cc-pVTZ level.[37] Our result agrees with recent experimental findings from far infrared laser absorption spectroscopy[39] that suggest a value higher than 88 cm^{-1} for the torsional fundamental frequency. The stack of energy levels, Table 3, shows the effect of the barrier. Near the bottom of the well the stack resembles an ordinary vibration, but close and above the barrier the behavior is similar to a free rotor. The distribution of energy levels is very different from a set of levels spaced 135 cm^{-1} as predicted by the harmonic approximation. Thus, an important effect can be expected on the calculated thermodynamic properties.

The a′ symmetry ν_7 mode corresponds to the O···O stretching.[36] A potential function was obtained from a grid of points on the O···O distance performed to both sides of the equilibrium position, 2.9108 Å. Thus, values from 2.3108 to 3.9108 Å in increments of 0.2 Å are used, including an additional point at 4.4108 Å. The remaining internal coordinates are fully optimized at each point. The kinetic term is fixed at the equilibrium value, $B_{OO} = 1.87$ cm^{-1}, because only changes of 10^{-3} cm^{-1} with the O···O distance are observed. The potential is obtained by a nonlinear least squares fit of the energy points to a Morse function on the displacement coordinate Δr_{OO}. The result is (in cm^{-1})

$$V = 1802.1.[1 - \exp(-1.38\Delta r_{OO})]^2 \quad (14)$$

with correlation $R = 0.99172$. The dissociation energy calculated from this potential is 5.15 kcal/mol. This result agrees with both the accepted experimental value, 5.44 ± 0.7 kcal/mol,[44] and the accurate estimate of the complete basis set dissociation energy, 5.0 ± 0.1 kcal/mol.[8a] Despite its simplicity, the Morse function seems to be able to produce reliable values for the dissociation energy of hydrogen complexes. This is also supported by the results obtained for the hydrogen fluoride

TABLE 2: Calculated, ν_{calc}, and Experimental, ν_{exp}, Frequencies for the Water Dimer[a]

mode	sym.	B	V_2	V_3	V_4	ν^b_{calc}	ν^c_{calc}	ν_{calc}	ν_{exp}
ν_{12}	a″	15.76	286.94			135	105[d]	140[e]	>88[g]
ν_{11}	a″	16.32	402.73			162		145[e]	
ν_8	a′	9.45	699.74	182.21	−39.34	163	158	157[e]	
ν_7	a′	8.72	1120.09			198	153[d]	186[e]	150[h]
ν_6	a′	15.23	2330.79	−723.47		377	371	354[e]	310,[i] 300[j]
ν_{10}	a″	16.18	6748.23		−2876.15	661	639	645[e]	520,[i] 500[j]
ν_5	a′	15.55	44380.74	−15915.00		1661	1654	1630[f]	1601,[i] 1593[j]
ν_4	a′	15.65	45455.52	14845.00		1687	1680	1651[f]	1619,[i] 1612[j]
ν_3	a′	16.02	222246.00			3773	3548[d]	3746[f]	3480[k]
ν_2	a′	16.14	230595.07	-396130.00	506393.00	3858	3803	3835[f]	3627,[l] 3634[m]
ν_1	a′	15.69	249624.02	−507745.00	827948.00	3958	3905	3938[f]	3699,[l] 3709[m]
ν_9	a″	15.58	253472.60		−995779.75	3974	3769	3957[f]	3715,[l] 3726[m]

[a] Kinetic terms at the equilibrium position, B, and potential functions ($V = V_2q^2 + V_3q^3 + V_4q^4$) are included. The V_2 terms correspond to the harmonic approximation. Symmetry referred to the C_s point group. All data in cm^{-1}. [b] Harmonic frequencies at the MP2(Full)/6-311++G(2d,2p) level, this work and refs 10 and 28a. [c] Anharmonic frequencies, this work. [d] Anharmonic frequencies calculated with the potentials of eqs 13, 14, and 12 and the kinetic terms presented in the text. [e] Harmonic frequencies computed at the MP2/aug-cc-pVTZ level.[37] [f] Harmonic frequencies computed at the MP2/[9,6,4,2/6,4,2] level.[38] [g] From tunable far infrared laser absorption spectroscopy.[39] [h] From electric resonance spectroscopy.[40] [i] Experimental data obtained in solid nitrogen matrix.[41] [j] Experimental data obtained in solid argon matrix.[41] [k] From coherent anti-Stokes Raman spectroscopy (CARS).[42] [l] Experimental data obtained in solid nitrogen matrix.[43] [m] Experimental data obtained in solid argon matrix.[43]

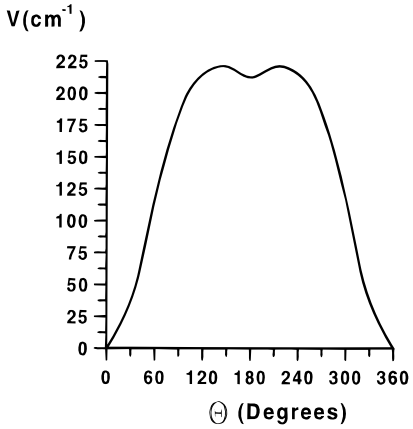

Figure 2. Potential energy curve for the torsion, ν_{12} mode, of the donor water monomer around the O···O axis in the water dimer.

TABLE 3: Calculated Torsional Energy Levels, in cm^{-1}, for the Water Dimer[a]

v_{12}	sym.	ν (cm^{-1})
0	a′	0
1	a″	105
2	a′	157
3	a′	228
4	a″	233
5, 6	a″	397
7, 8	a′, a″	634
9, 10	a′, a″	942
11, 12	a′, a″	1318

[a] The first energy level is placed at 62 cm^{-1} of the potential well. The first column corresponds to a pure vibrational quantum number. Symmetry referred to the C_s point group.

dimer[26] where the Morse function predicted a dissociation energy that only differs by 0.07 kcal/mol from the experimental estimate. The energy levels for this mode will be obtained as

$$\nu = \nu_e(v + {}^1/_2) - \nu_e\chi_e(v + {}^1/_2)^2 \qquad (15)$$

with

$$\nu_e = 2\sqrt{D_e a^2 B_{OO}}$$
$$\chi_e = \nu_e/4D_e \qquad (16)$$

where v represents the vibrational quantum number, B_{OO} is the kinetic term, D_e is the dissociation energy, and a is the exponential factor in the Morse potential. Table 2 shows that the calculated fundamental frequency, 153 cm^{-1}, is in good agreement with the experimental value,[40] 150 cm^{-1}. The result is closer to the observed frequency than the harmonic results obtained at higher levels of theory, see Table 2.

The anharmonic corrections for the remaining low-frequency modes, ν_{11}, ν_8, ν_6, and ν_{10}, are obtained using displacements along the normal modes. For these soft modes, large increments of the normal coordinate are needed to describe the potential surface. Therefore, we obtain large cubic and quartic corrections that generate spurious potential minima. Thus, it is necessary to limit the size of the basis in the variational treatment to describe the zone of interest, and only the lowest energy levels are correctly obtained. So, in this work only the fundamental frequencies will be corrected. This problem is specially important for the ν_{11} mode. We have found that even anharmonic potentials previously proposed for this mode[10] experience the same problem. Thus, no correction is introduced in this case. For the ν_6 mode it is possible to generate an anharmonic correction using displacements of ±0.25 and ±0.5 on the normal coordinate. The ν_8 and ν_{10} modes are considered using normal modes expressed in internal coordinates[34] with displacements of ±2 and ±1.5 respectively. The resulting kinetic terms, potential functions, and fundamental frequencies, calculated variationally in the harmonic oscillator basis, are shown in Table 2. The calculated frequencies are similar to the results obtained at much higher level of theory, see Table 2.

The coupling between the O···O stretching (ν_7 mode) and the bridge O−H stretching (ν_3 mode) of the water dimer is usually investigated by generating a two-dimensional model with the O···O and O−H distances as vibrational coordinates. Here, we analyze the reliability of this approach constructing a two dimensional model, including kinetic and potential interactions. Thus, a grid of points from 2.5108 to 3.9108 Å and from 0.9242 to 1.0442 Å is performed on the O···O and O−H coordinates using increments of 0.4 Å. The coordinates not involved in the grid are fully optimized at each point. The kinetic terms are calculated through the elements of the rotational−vibrational **G** matrix.[16,17] The variation with the vibrational coordinates for the B_{OO}, $B_{OO,OH}$, and B_{OH} kinetic elements is found very small. Thus, the equilibrium values, 1.929, 0.986, and 17.689 cm^{-1}, are selected. An analytical function for the potential is obtained by fitting the energy data to a double Taylor series

TABLE 4: Variation of Entropy, Enthalpy and Equilibrium Constant for the Reaction of Formation of the Water Dimer[a]

property	case a[b]	case b[c]	case c[d]	case d[e]	expt[f]
ΔS (cal/(mol·K))	−20.98	−19.87	−19.83	−19.48	−18.59 ± 1.30
ΔH (kcal/(mol·K))	−2.24	−3.08	−3.15	−3.06	−3.59 ± 0.5
K_p (atm^{-1})	0.0005	0.0029	0.0032	0.0034	0.0110

[a] Data at 373 K and at a constant pressure of 1 atm. The refined partition function of the monomer is used in all the cases. [b] Calculated with eq 5 using the harmonic frequencies for the water dimer. [c] Calculated with eq 5 using the anharmonic frequencies for the water dimer. [d] Calculated with direct summation of energy levels for the torsion, ν_{12}, mode. The remaining modes are included with eq 5 using the anharmonic frequencies. [e] Calculated with direct summation of energy levels for the torsion, ν_{12}, and O···O stretching, ν_7, modes. The remaining modes are included with eq 5 using the anharmonic frequencies. [f] Experimental data estimated from thermal conductivity measurements.[44]

expansion on the vibrational coordinates. Thus, we get (in cm^{-1})

$$V = 4492.06(\Delta r_{OO})^2 - 6402.05(\Delta r_{OO})^3 + 2932.41(\Delta r_{OO})^4 + 198\,791.32(\Delta r_{OH})^2 - 381\,040.61(\Delta r_{OH})^3 - 139\,383.44(\Delta r_{OH})^4 - 866.44(\Delta r_{OO})(\Delta r_{OH}) + 2367.67(\Delta r_{OO})^2(\Delta r_{OH}) + 2206.79(\Delta r_{OH})^2 \quad (17)$$

with correlation $R = 0.999\,93$ and standard deviation $\sigma = 14.31$ cm^{-1}. The vibrational energy levels are computed variationally in a double harmonic oscillator basis. The fundamental frequencies for the O···O and the O−H stretching modes are found to be 176 and 3321 cm^{-1}, respectively. These data can be compared to the corresponding 198 and 3773 cm^{-1} harmonic values and to the anharmonic one-dimensional results, 153 and 3548 cm^{-1}, see Table 2. The two-dimensional fundamental frequency for the O···O stretching is higher than the one-dimensional value but is still closer to the experimental result than the value obtained at the MP2/aug-cc-pVTZ level, see Table 2. On the other hand, the two-dimensional fundamental frequency for the O−H stretching is smaller than the experimental value. This fact can be explained decomposing the normal mode in internal coordinates. Thus, the Boatz and Gordon decomposition[34] is applied with GAMESS[3a] using the Hessian computed at the equilibrium position. The results show that the symmetric O−H stretching mode, ν_3, includes both the variation of the bridge O−H bond and the variation of the free donor O−H bond in a proportion of 3:1. Thus, this mode can only be approximately described by a single internal coordinate. However, the Boatz and Gordon decomposition[34] shows that the O···O stretching mode, ν_7, is mainly composed of the O···O distance. In this work we will use the one-dimensional results for the ν_3 and ν_7 modes because they seem to be more reliable.

Dimerization Reaction. For the dimerization reaction of water

$$2H_2O(g) \leftrightarrows (H_2O)_2(g) \quad (18)$$

the equilibrium constant can be obtained as[2]

$$\ln K_p = \ln q_D - 2\cdot\ln q_M + \ln N_a + D_e/RT \quad (19)$$

where q_M and q_D represent the molecular partition functions for the water monomer and dimer respectively, D_e represents the association energy, and N_a is Avogadro's constant. To compare with the available experimental data, K_p, ΔS and ΔH have been calculated at 373 K and at a constant pressure of 1 atm. The effect of anharmonicity on the thermodynamic properties is analyzed using the refined partition function of the monomer, $D_e = 5.15$ kcal/mol, and a ln q_D obtained in four different cases. The first and second cases are obtained applying eq 5 with the harmonic and anharmonic data of Table 2, respectively. The third case uses the anharmonic data of Table 2 except the torsion, ν_{12} mode, which is introduced in the partition function as a summation of the torsional levels collected in Table 3. The last case is similar to the third but also introduces the O···O stretching as a summation of the one-dimensional energy levels obtained with eq 15. In Table 4 the results are compared to the experimental data.

Case a of Table 4 shows that the harmonic picture yields a much smaller K_p than the experimental value. Inclusion of the anharmonic corrections, cases b, c, and d of Table 4, increases uniformly the ΔS and K_p values and approaches the experimental estimates. Cases b and c of Table 4 show a decrease of ΔH with respect to the pure harmonic case. Inclusion of the O···O stretching levels, case d, is reflected in an increase from the previous estimate, case c. Table 4 shows that these findings favor, in absolute terms, the upper limit of ΔS and the lower limit of ΔH experimental estimates. This behavior of ΔH has been observed by Feyereisen et al.[8a] from a harmonic model where anharmonicity in some low-frequency modes is introduced by halving the fundamental frequency. The smaller value obtained by these authors for ΔS can be attributed to the simplicity of the anharmonic treatment for the low-frequency vibrations. Our most accurate result for K_p, 0.0034 atm^{-1}, case d of Table 4, is smaller than the experimental value,[44] 0.0110 atm^{-1}. This discrepancy could be attributed to the use of the harmonic oscillator closed form, eq 5, for the anharmonic ν_{11}, ν_8,ν_6, and ν_{10} modes. This fact would be reflected in a contribution to K_p smaller than expected because the energy levels of an anharmonic oscillator are closer than in the harmonic picture. An estimate of the contribution to K_p of these modes can be obtained as follows. We can assume a contribution from each mode equal to the increase, 0.0002 atm^{-1}, observed in case d of Table 4 when the direct summation of the O···O stretching energy levels is added to case c of Table 4. Thus, the four anharmonic modes yield $K_p = 0.0042$ atm^{-1}, a result still smaller than the experimental. Although the present work is not accurate enough for a quantitative conclusion, the higher K_p found experimentally could, to some extent, be associated to the assumptions used in the experimental work.[44] Our results together with the findings of Feyereisen et al.[8a] suggest the utility of more accurate experimental studies to firmly establish the ΔS, ΔH, and the K_p values.

An analytical expression for the variation of K_p with temperature can be derived from eq 19. Therefore, a canonical partition function for the dimer is obtained using temperatures from 273.15 to 373.15 K at a constant pressure of 1 atm using the conditions of case d of Table 4. Using the monomer and dimer partition functions and eq 19 we get

$$\ln K_p = -10.27 + 1595.29/T + 162\,015\,58.49/T^3 \quad (20)$$

Figure 3 shows how the difference between the calculated and the experimental K_p decreases with temperature. This is a consequence of the population of energy levels. Both curves show the same high-temperature limit that, from eq 20, is found to be $3.47\ 10^{-5}$ atm^{-1}.

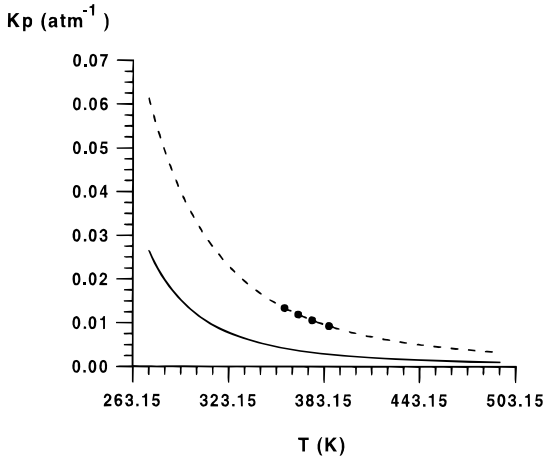

Figure 3. Variation with temperature of the equilibrium constant, K_p, for the dimerization reaction of water. The solid line corresponds to the theoretical results obtained in this work. The dashed line is obtained fitting the experimental data available[44] (represented by dots) to a third-order polynomial form on $1/T$.

Conclusions

The effect of anharmonicities on the thermodynamic properties of water dimerization is studied using a statistical model. Inclusion of anharmonicities into the model for the water monomer is not reflected in a significant change of the C_p and S values. However, in the cases of the internal and Gibbs energies the difference reaches 0.47 kcal/mol. In the water dimer, anharmonic corrections are introduced to the vibrational modes. In particular, the torsional motion of the donor molecule around the O···O axis in the water dimer is fully analyzed for the first time. The fundamental frequency for this torsional mode is found to be 105 cm^{-1}. This result agrees with the experimental evidence for a value[39] higher than 88 cm^{-1}. The barrier to internal rotation is estimated in 221 cm^{-1}.

The dissociation energy of the water dimer, obtained by fitting the O···O stretching mode to a Morse oscillator, is found to be 5.15 kcal/mol. This result agrees with the experimental value 5.44 ± 0.7 kcal/mol[44] and the theoretical complete basis set result estimated at 5.0 ± 0.1 kcal/mol.[8a] The fundamental frequency of vibration is estimated to be 153 cm^{-1}, in agreement with the experimental value,[40] 150 cm^{-1}.

The reliability of the usual two-dimensional model, which uses internal coordinates, for the symmetric OH stretching of the water donor and the O···O stretching is investigated. Using this model, we found that the calculated fundamental frequency for the OH mode underestimates the experimental result. This discrepancy arises from the composition of the symmetric OH stretching mode, which is only approximately described by the OH bond length. Thus, this type of two-dimensional model gives only a qualitative description of the coupling between the hydrogen bond stretching modes.

The effect of anharmonicity in ΔS, ΔH, and the K_p constant for the dimerization reaction is investigated. The inclusion of anharmonic corrections favors, in absolute terms, the upper limit of ΔS and the lower limit of ΔH experimental estimates whereas the K_p value approaches the experimental result. However, our best estimate for K_p is smaller than the experimental one. This fact is probably caused by the lack of interaction in the vibrational model. Finally, it is found that the difference between the calculated and experimental K_p values decreases with temperature. The high-temperature limit is estimated to be 3.47×10^{-5} atm^{-1}.

Acknowledgment. The authors thank the DGICYT (Project No. PB93-0142-C03-03) and the Universidad de Castilla-La Mancha for financial support.

References and Notes

(1) Del Bene, J. E. *Molecular Structure and Energetics. Vol. 1, Chemical Bonding Models*; Liebman, J. F.; Greenberg, A., Eds.; VCH Publishers, Inc: New York, 1986; Chapter 9.

(2) (a) McQuarrie, D. A. *Statistical Mechanics*; Harper & Row: New York, 1973. (b) Lucas, K. *Applied Statistical Thermodynamics*; Springer-Verlag: New York, 1991.

(3) (a) Schmidt, M. W.; Baldridge, K. K.; Boatz, J. A.; Elbert, S. T.; Gordon, M. S.; Jensen, J. H.; Koseki, S.; Matsunaga, N.; Nguyen, K. A.; Su. S.; Theresa, L. W.; Dupuis, M.; Montgomery, J. A., Jr. GAMESS. *J.* Comput. *Chem.* **1993**, *14*, 1347−1363. (b) Frisch, M. J.; Trucks, G. W.; Schlegel, H. B.; Gill, P. M. W.; Johnson, B. G.; Robb, M. A.; Cheeseman, J. R.; Keith, T. A.; Petersson, G. A.; Montgomery, J. A.; Raghavachari, K.; Al-Laham, M. A.; Zakrzewski, V. G.; Ortiz, J. V.; Foresman, J. B.; Cioslowski, J.; Stefanov, B. B.; Nanayakkara, A.; Challacombe, M.; Peng, C. Y.; Ayala, P. Y.; Chen, W.; Wong, M. W.; Andres, J. L.; Replogle, E. S.; Gomperts, R.; Martin, R. L.; Fox, D. J.; Binkley, J. S.; Defrees, D. J.; Baker, J.; Stewart, J. P.; Head-Gordon, M.; Gonzalez, C.; Pople, J. A. *Gaussian 94*, Revision B.3; Gaussian, Inc.: Pittsburgh, PA, 1995.

(4) (a) Serre, J. *Adv. Quantum Chem.* **1974**, *8*, 1−36. (b) Longuet-Higgins, H. C. *Mol. Phys.* **1963**, *6*, 445−460.

(5) Wilson, E. B., Jr.; Decius, J. C.; Cross C. *Molecular Vibrations*; Dover Publications, Inc.: New York, 1980. Republication of the original work of 1955 published by McGraw-Hill Book Company, Inc., New York.

(6) (a) Smith, B. J.; Swanton, D. J.; Pople, J. A.; Schaefer, H. F., III; Radom, L. *J. Chem. Phys.* **1990**, *92*, 1240−1247. (b) Scheiner, S. *Reviews in Computational Chemistry*; Lipkowitz, K. B., Boyd, D. B., Eds.; VCH Publishers, Inc: New York, 1991; Vol. II, Chapter 5. (c) Scheiner, S. *Annu. Rev. Phys. Chem.* **1994**, *45*, 23−56.

(7) Curtiss, L. A.; Blander, M. *Chem. Rev.* **1988**, *88*, 827−841.

(8) (a) Feyereisen, M. W.; Feller, D.; Dixon, D. A. *J. Phys. Chem.* **1996**, *100*, 2993−2997. (b) Althorpe, S. C.; Clary, D. C. *J. Chem. Phys.* **1995**, *102*, 4390−4399. (c) Xantheas, S. S. *J. Chem. Phys.* **1994**, *100*, 7523−7534. (d) Coker, D. F.; Watts, R. O. *J. Phys. Chem.* **1987**, *91*, 2513−2518.

(9) Curtiss, L. A.; Frurip, D. J.; Blander, M. *J. Phys. Chem.* **1982**, *86*, 1120−1125.

(10) Kim, K. S.; Mhin, B. J.; Choi, U; Lee, K. *J. Chem. Phys.* **1992**, *97*, 6649−6662.

(11) (a) Del Bene, J. E.; Mettee, H. D.; Frisch, M. J.; Luke, B. T.; Pople, J. A. *J. Phys. Chem.* **1983**, *87*, 3279−3282. (b) van Duijneveldt-van de Rijdt, J. G. C. M.; van Duijneveldt, F. B. *J. Chem. Phys.* **1992**, *97*, 5019−5030.

(12) Maréchal, Y. *Molecular Interactions*; Ratajczak, H., Orville-Thomas, W. J., Eds.; Wiley: New York, 1980; Vol. 1, Chapter 8.

(13) Sandorfy, C. *Top. Curr. Chem.* **1984**, *120*, 41−84.

(14) (a) Robertson, G. N. *Philos. Trans. R. Soc. London A.* **1977**, *286*, 25−53. (b) Bouteiller, Y.; Mijoule, C.; Karpfen, A.; Lischka, H.; Schuster, P. *J. Phys. Chem.* **1987**, *91*, 4464−4466.

(15) Pickett, H. M. *J. Chem. Phys.* **1972**, *56*, 1715−1723.

(16) Harthcock, M. A.; Laane, J. *J. Phys. Chem.***1985**, *89*, 4231−4240.

(17) Niño, A; Muñoz-Caro, C. *Comput. Chem.* **1994,** *18*, 27−32.

(18) Szabo, A.; Ostlund, N. S. *Modern Quantum Chemistry*; Mc Graw Hill, Inc.: New York, 1989; pp 43−45.

(19) (a) Smeyers, Y. G.; Niño, A.; Moule, D. C. *J. Chem. Phys.* **1990**, *93*, 5786−5795. (b) Ozkabak, A. G.; Philis, J. G.; Goodman, L. *J. Am. Chem. Soc.* **1990**, *112*, 7854−7860. (c) Ozkabak, A. G.; Goodman, L. *J. Chem. Phys.* **1992**, *96*, 5958−5968. (d) Smeyers, Y. G.; Senent, M. L.; Botella, V.; Moule, D. C. *J. Chem. Phys.* **1993**, *98*, 2754−2767. (e) Goodman, L.; Kundu, T.; Leszczynski, J. *J. Phys. Chem.* **1996**, *100*, 2770−2783.

(20) Muñoz-Caro, C.; Niño, A.; Moule, D. C. *Chem. Phys.* **1994**, *186*, 221−231.

(21) Niño, A.; Muñoz-Caro, C.; Moule, D. C. *J. Phys. Chem.* **1995**, *99*, 8510−8515.

(22) Niño, A.; Muñoz-Caro, C.; Moule, D. C. *J. Phys. Chem.* **1994**, *98*, 1520−1524.

(23) Muñoz-Caro, C.; Niño, A.; Moule, D. C. *J. Mol. Struct.* **1994**, *350*, 83−89.

(24) Niño, A.; Muñoz-Caro, C. *Comput. Chem.* **1995**, *19*, 371−378.

(25) (a) Bartlett, R. J.; Cole, S. J.; Purvis, G. D.; Ermler, W. C.; Hsieh, H. C.; Shavitt, I. *J. Chem. Phys.* **1987**, *87*, 6579−6591. (b) Zhang, N. R.; Shillady, D. D. *J. Chem. Phys.* **1994**, *100*, 5230−5236.

(26) Niño, A.; Muñoz-Caro, C. *Comput. Chem.* **1997**, *21*, 143−151.

(27) Fletcher, R. *Practical Methods of Optimization*; John Wiley & Sons: New York, 1987; Reprinted 1990; Chapter 3.

(28) (a) Frisch, M. J.; Del Bene, J. E.; Schaefer, H. F., III *J. Chem. Phys.* **1986**, *84*, 2279−2289. (b) Bertran, J.; Ruiz-López, M. F.; Rinaldi, D.; Rivail, J. L. *Theor. Chim. Acta* **1992**, *84*, 181−194. (c) Mó, O.; Yáñez, M.; Rozas, I.; Elguero, J. *Chem. Phys. Lett.* **1994**, *219*, 45−52.

(29) Muñoz-Caro, C.; Niño, A. *QCPE Bull.* **1993**, *13*, 4.
(30) Muñoz-Caro, C.; Niño, A. *QCPE Bull.* **1995**, *15*, 48.
(31) Niño, A.; Muñoz-Caro, C. *QCPE Bull.* **1997**, *17*, 1.
(32) Feller, D.; Feyereisen, M. W. *J. Comput. Chem.* **1993**, *14*, 1027−1035.
(33) Pople, J. A.; Schlegel, H. B.; Krishnan, R.; Defrees, D. J.; Binkley, J. S.; Frisch, M. J.; Whiteside, R. A.; Hout, R. F.; Hehre, W. J. *Int. J. Quantum Chem.* **1981**, *15*, 269−278.
(34) Boatz, J. A.; Gordon, M. S. *J. Phys. Chem.* **1989**, *93*, 1819−1826.
(35) *CRC Handbook of Chemistry and Physics;* Weast, R. C., Ed.; CRC Press: Boca Raton, FL, 1981.
(36) Reimers, J.; Watts, R. O. *Chem. Phys.* **1984**, *85*, 83−112.
(37) Xantheas, S. S.; Dunning, T. H., Jr. *J. Chem. Phys.* **1993**, *99*, 8774−8792.
(38) Kim, J.; Lee, J. Y.; Lee, S.; Mhin, B. J.; Kim, K. S. *J. Chem. Phys.* **1995**, *102*, 310−317.
(39) Pugliano, N.; Cruzan, J. D.; Loeser, J. G.; Saykally, R. J. *J. Chem. Phys.* **1993**, *98*, 6600−6617.
(40) Dyke, T. R.; Mack, K. M.; Muenter, J. S. *J. Chem. Phys.* **1977**, *66*, 498−510.
(41) Yeo, G. A.; Ford, P. A. *Struct. Chem.* **1992**, *3*, 75−93.
(42) Wuelfert, S.; Herren, D.; Leutwyler, S. *J. Chem. Phys.* **1987**, *86*, 3751−3753.
(43) (a) Amos, R. D. *Chem. Phys.* **1986**, *104*, 145−151. (b) Bentwood, R. M.; Barnes, A. J.; Orville-Thomas, W. J. *J. Mol. Spectrosc.* **1980**, *84*, 391−404.
(44) Curtiss, L. A.; Frurip, D. J.; Blander, M. *J. Chem. Phys.* **1979**, *71*, 2703−2711.